ELECTRODEPOSITION OF PERMALLOY IN DEEP SILICON TRENCHES WITHOUT EDGE-OVERGROWTH UTILIZING DRY FILM PHOTORESIST

Sang-Won Park, Debbie G. Senesky, and Albert P. Pisano
Berkeley Sensor and Actuator Center (BSAC)
University of California, Berkeley, California 94720, USA

ABSTRACT

An electrodeposition process for embedding NiFe alloys in deep silicon trenches (100 µm) without edge-overgrowth was developed by utilizing dry film photoresist as a sacrificial trench top. The dry film photoresist prevented high concentration of current flux at the trench edges during electrodeposition leading to planar deposition topographies. In addition, the effect of the applied current density on material composition of the electrodeposited NiFe film was investigated, and the composition for permalloy ($Ni_{80}Fe_{20}$) was obtained with a current density of 100 mA/cm^2. Furthermore, the B-H response of the electrodeposited permalloy films exhibited a saturation magnetic flux density and relative permeability of 1.23 Tesla and 82, respectively. The electrodeposition technique developed in this work was utilized to fabricate a free-standing MEMS electromagnetic linear actuator composed of silicon and permalloy structures.

INTRODUCTION

Ferromagnetic materials embedded in silicon have been utilized to develop Microelectromechanical System (MEMS) devices [1]. For example, MEMS researchers have utilized ferromagnets to develop microactuators, sensors and micromotors because of the ability to produce high force and large stroke electromagnetic actuation [2-4]. The most commonly used ferromagnetic material is permalloy ($Ni_{80}Fe_{20}$) due to its superior magnetic properties and manufacturability. Permalloy is known for its high permeability, high magnetic saturation, low coactivity, good corrosion resistance and near-zero magnetostriction [5]. In addition, low stress deposition processes have been developed to obtain film thicknesses between a few nanometers and millimeters [6, 7].

Electrodeposition is a fabrication technique that is often used to deposit permalloy. This technique has the advantage of obtaining high growth rate while maintaining low film stress; unlike evaporation and sputtering techniques [8]. In addition, selective growth can be obtained to create isolated features that can be embedded or released to create microstructures. Furthermore, the magnetic and physical properties of electrodeposited films can be altered by adjusting deposition parameters such as current density, temperature and pH of electrolyte [1, 7, 9].

The drawback of the electrodeposition process is non-uniform deposition topography in trenches which requires planarization techniques. The deposition profile of electrodeposited material within a trench is affected by the geometrical configuration. More specifically, the large area of the anode in comparison to the cathode (deposition surface) causes crowding of the electric field at the top perimeter of the trench. In Figure 1, the results of a finite element modeling (FEM) analysis are shown to observe the current flux density distribution during electrodeposition inside of an isolated silicon trench. The simulation demonstrates a high concentration of current flux at the top trench edge surface. This high concentration of current flux causes an increased growth rate at the edge of the trench, leading to edge-overgrowth. In many fabrication sequences, a planar topography is necessary for lithography steps, and etchback methods such as chemical mechanical polishing (CMP), mechanical lapping or reverse electroplating are often utilized [10, 11]. However, these techniques reduce the fabrication throughput leading to higher manufacturing costs.

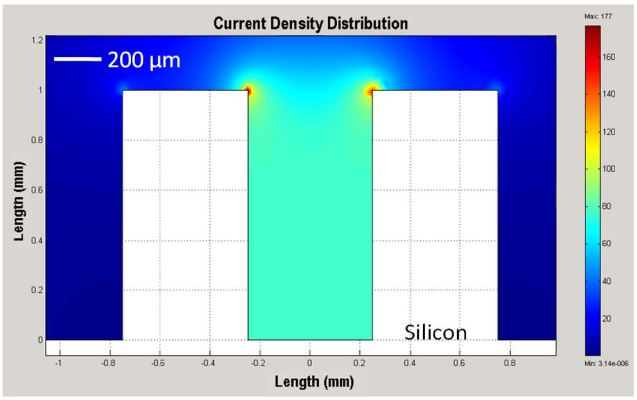

Figure 1: The FEM analysis was performed to simulate the current flux density distribution inside of an isolated trench during electrodeposition. The simulation demonstrates high flux concentration at the top edges of the trench, which causes edge-overgrowth.

This paper presents fabrication technology for the electrodeposition of thick (above 100 µm) material without edge-overgrowth through the utilization of dry film photoresist as a sacrificial trench top. The technology can be used for applications that utilize electrodeposition processes such as electrical interconnects or MEMS structures. The advantage of this process is an elimination of the etchback process, which is typically employed to remove the edge-overgrowth material. In addition to the deposition topography, the material properties such as composition, relative permeability and saturation flux density of electrodeposited permalloy films are investigated.

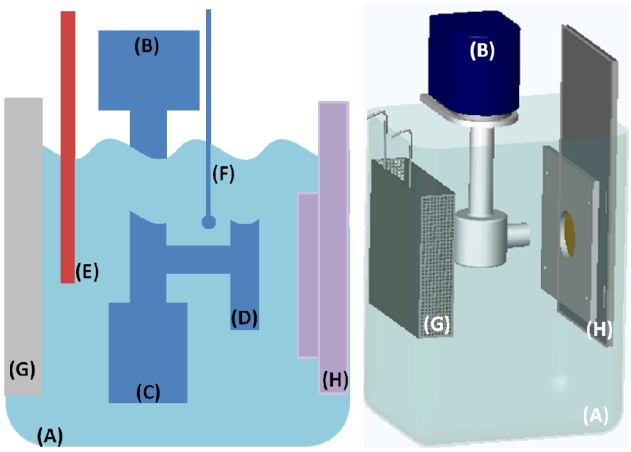

Figure 2: The schematic of NiFe alloy electrodeposition apparatus. (A) 10 liter chromatography jar, (B) Pump, (C) Filter, (D) Multi-holes nozzle, (E) Immersion heater, (F) Temperature probe, (G) Ni basket (Anode) and (H) Sample holder (Cathode).

EXPERIMENTAL

Electrodeposition Apparatus

A citrate-complexed NiFe electrolyte was utilized for electrodeposition as it has demonstrated deposition of thin films with superior magnetic properties during long electrodeposition times (up to approximately 25 hours) and insensitivity to deviations in deposition parameters (current density, pH and temperature) [7, 9]. The electrolyte is composed of 112 g/l of nickel sulfate ($NiSO_4 \cdot 6H2O$), 5 g/l of iron sulfate ($FeSO_4 \cdot 7H2O$), 75 g/l of sodium citrate ($Na_3C_6H_5O_7 \cdot 2H_2O$), 1.5 g/l of potassium sulfate (K_2SO_4), 0.2 g/l of sodium n-dodecyl sulfate ($C_{12}H_{15}SO_4Na$) and 1 g/l of saccharin ($C_7H_5NO_3S$). Sodium n-dodecyl sulfate is an anionic surfactant compound which promotes wetting of the cathode surface, and saccharin is utilized as a stress reducing agent [7]. A schematic of electroplating apparatus is shown in Figure 2. A 10 liter chromatography jar (A) holds electrolyte while a pump (B) agitates the electrolyte through a filter (C). Direct impingement of the electrolyte into the surface of the sample is achieved by a nozzle with multiple holes (D). A constant electrolyte temperature of 45ºC is obtained by a temperature controller, which is coupled with an immersion heater (E) and a temperature probe (F). A titanium anode basket (G) holds electrolytic nickel rounds and is covered by an anode bag filter, which prevents nickel particulates from depositing on the sample surface. A cathode sample holder (H) fixtures the sample inside the electrodeposition cell, providing a consistent sample location. A power supply with current control provides a current flow between the anode and the cathode and initiates electron transfer. The current density has been shown to affect the film depostion rate and composition [7], and a constant current source, therefore, was utilized to aid in obtaining a uniform composition through the depth of the deposit.

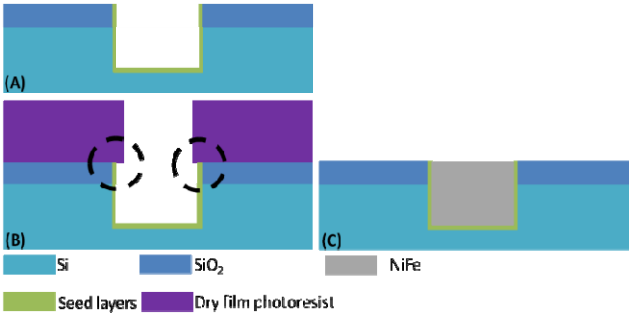

Figure 3: Fabrication process implemented to prevent edge-overgrowth utilizing dry film photoresist as a sacrificial trench top. (A) Conductive seed layers (chromium/copper) were evaporated onto a 100 µm deep trench, (B) Dry film photoresist was deposited and patterned and (C) Electrodeposition of NiFe film was performed followed by lift-off of the dry film photoresist layer.

Fabrication Process

The characterization of electrodeposited NiFe alloys during trench filling was performed by utilizing trenches, which were etched into a silicon substrate (Figure 3). Thermal silicon dioxide film (1 µm thick) was grown on top of a 500 µm thick silicon substrate, and trenches (100 µm deep and 500 µm wide) were anisotropically etched with a Deep Reactive Ion Etching (DRIE) process. Thin films of chromium and copper were deposited sequentially with an E-beam evaporator to obtain thicknesses of 50 nm and 200 nm, respectively (Figure 3, (A)). The chromium film serves as an adhesion layer between the silicon substrate and the copper seed layer. In order to prevent edge-overgrowth, a 40 µm thick dry film photoresist (Riston FX-940) was deposited on top of the substrate (Figure 3, (B)). Deposition of the dry film photoresist serves as a sacrificial trench top for the prevention of edge-overgrowth. The dry film photoresist was then patterned with photolithography. A 15 µm overhang of dry film photoresist was utilized to accommodate misalignment errors during the photolithography process and ensured complete coverage of the trench sidewalls. An additional benefit of employing of the dry film photoresist is the selective electrodeposition across the wafer; the dry film photoresist masks the selected regions of silicon surface preventing electrodeposition. In addition, unlike liquid photoresist, dry film photoresist has non-conformal wafer coverage and enables lithography above pre-existing features. Upon patterning of the dry film photoresist, timed electrodeposition of NiFe alloy into the trench is followed (Figure 3, (C)). Finally, lift-off of the sacrificial dry film photoresist was performed with an acetone etch to reveal surface of the silicon substrate.

RESULTS

Deposition Topography

To characterize the topography of the electrodeposited NiFe structures, the electroplating was performed in silicon trenches with and without deposition of sacrificial dry film photoresist.

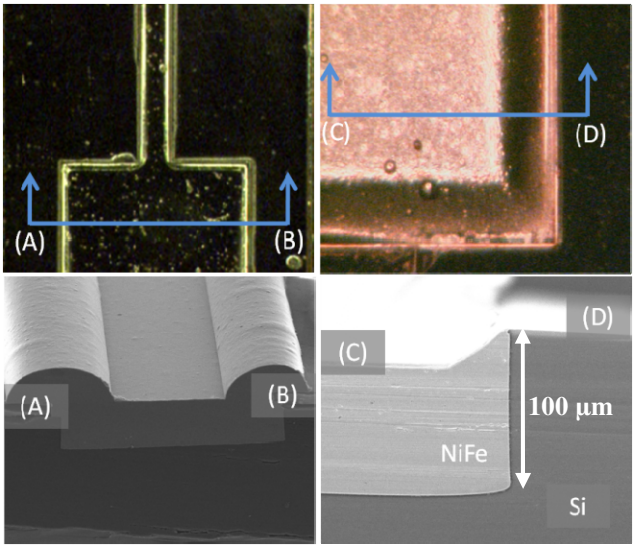

Figure 4: Microscope and SEM images of the top and cross sectional views for the topography of electrodeposited NiFe structures in silicon trenches. (A)-(B) topography of electrodeposition without dry film photoresist demonstrating edge-overgrowth and (C)-(D) topography of electrodeposition that utilized the sacrificial dry film photoresist demonstrating prevention of edge-overgrowth.

Microscope and Scanning Electron Microscope (SEM) images of the deposition topographies and cross sections are shown in Figure 4. The deposition profile in the trench without the dry film photoresist (Figure 4, (A)-(B)) shows edge-overgrowth as was predicted in the FEM analysis. In contrast, the deposition profile in the trench that utilized the dry film photoresist (Figure 4, (C)-(D)) demonstrates no edge-overgrowth and a planar topography. In both cases, good trench filling was demonstrated; no voids or pinholes were observed. The thickness of the embedded NiFe structure was measured to be approximately 100 µm. In addition, the electroplated trench structure utilizing the dry film photoresist demonstrated a lower deposition rate compared with the trench deposition without the dry film photoresist even with identical deposition conditions.

Material Properties

The material composition of electrodeposited NiFe films for various applied current densities was measured (Figure 5). Previous work has shown that the composition of electrodeposited NiFe alloys can be controlled with the applied current density [7, 12]. In this work, Energy Dispersive X-ray (EDX) spectrum analysis was performed to obtain the nickel and iron concentrations of the electrodeposited NiFe films. As shown in Figure 5, a decrease of iron weight percentage was observed with respect to an increase in the applied current density. Furthermore, the figure demonstrates that the composition of permalloy ($Ni_{80}Fe_{20}$) was achieved with an applied current density of approximately 100 mA/cm^2.

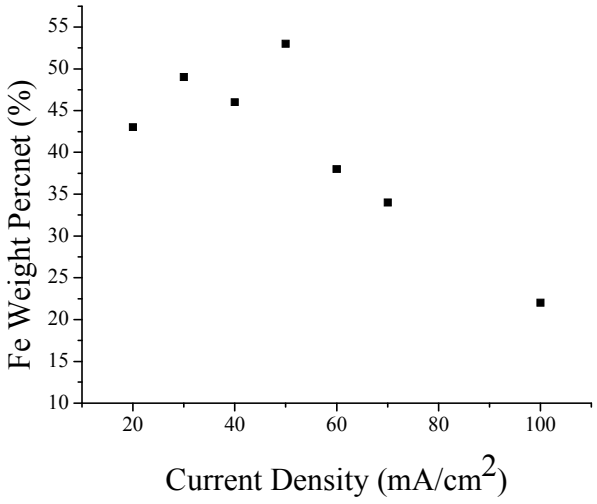

Figure 5: Weight percent of iron for various NiFe films with respect to the applied current density during electrodeposition. Permalloy composition ($Ni_{80}Fe_{20}$) was achieved with applied current density of 100 mA/cm^2.

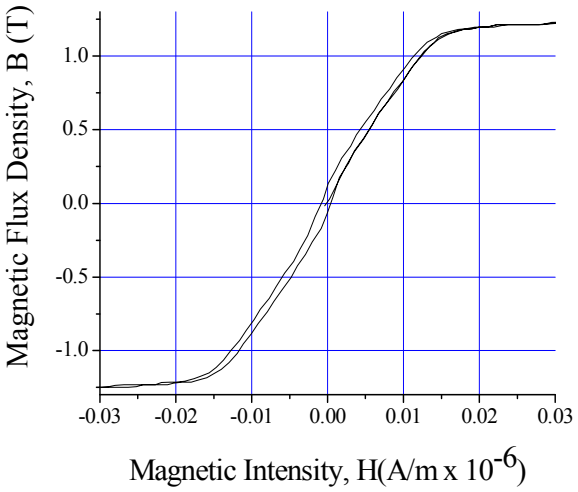

Figure 6: The B-H response of 100 µm thick electrodeposited permalloy film showing a saturation magnetic flux density of 1.23 Tesla and relative permeability as 82 of B = 0.4 Tesla.

In addition to the film composition, the magnetic properties of the 100 µm thick electrodeposited permalloy structure were characterized. The B-H response of the sample was measured and is shown in Figure 6. The saturation magnetic flux density (B_s) of the permalloy sample was measured to be approximately 1.23 Tesla. In addition, the relative permeability (μ_r) was determined as approximately 82 at magnetic flux density of 0.4 Tesla. It should be noted that the measured saturation flux density agrees with previously reported values of 1.18 Tesla for permalloy films [13].

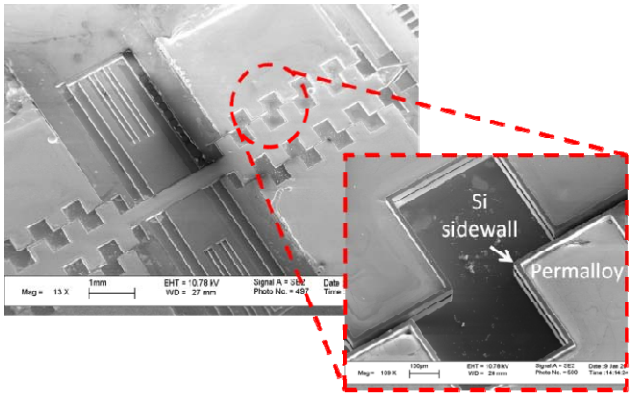

Figure 7: The electrodeposition process with the utilization of dry film photoresist as a sacrificial trench top was utilized to fabricate a MEMS electromagnetic linear actuator composed of silicon and permalloy structures. The permalloy structure was electrodeposited inside of silicon trenches without edge-overgrowth.

However, the relative permeability obtained in this work is higher than the previously reported work, which demonstrated the minimum relative permeability of 50 with permalloy films thickness of 70 µm. [13]. The contrasting values are affected by the variation in the reference flux used during the B-H measurement and the stress properties of the films.

Device Fabrication

The electrodeposition process described above was utilized to fabricate a MEMS electromagnetic linear actuator (Figure 7). The integration of post processing steps that include photolithography and DRIE were utilized to define features in the silicon mold. More specifically, the mechanical flexures, armature and stator of the MEMS electromagnetic linear actuator were defined. In addition, a releasing step was used to free the composite silicon and permalloy device. The deposition profile of the permalloy structure with a thickness of 100 µm showed no edge-overgrowth leading to a planar topography that enables photolithography without post-etchback steps. In addition, the release of closely-packed features was accomplished to create an actuatable, free-standing electromagnetic device.

CONCLUSION

A unique electrodeposition method to embed NiFe alloy structures in silicon was developed through the utilization of dry film photoresist as a sacrificial trench top. The dry film photoresist served as a temporary mask, which prevents high deposition rate at the trench edges. This process demonstrated the prevention of edge-overgrowth; eliminating the need for post planarization or etchback steps. The material composition of NiFe alloys with respect to applied current density was investigated, and permalloy composition was obtained with a current density of 100 mA/cm^2. In addition, the B-H response of permalloy structures (100 µm thick) was measured and showed a saturation magnetic flux density and relative permeability of 1.23 Tesla and 82, respectively. Furthermore, the feasibility of this process to create free-standing MEMS structures was demonstrated through the fabrication of a composite MEMS electromagnetic linear actuator. The prevention of edge-overgrowth enabled planar topographies, which are necessary for photolithography used to define structural features.

REFERENCES

[1] N.V. Myung, D.-Y. Park, B.-Y. Yoo, and T.A. Paulo, "Development of electroplated magnetic materials for MEMS," *Magnetism and Magnetic Materials*, vol. 265, 2003, pp. 189-198.

[2] Z. Cui, X. Wang, Y. Li, and G.Y. Tian, "Fabrication of micromirror-based magnetic sensor," *J. Phys.: Conf. Ser,* vol. 76, 2007.

[3] C.T. Pan, and S.C. Shen, "Magnetically actuated bi-directional microactuators with permalloy and Fe/Pt hard magnet," *J. Magnetism and Magnetic Materials*, vol. 285, no. 3, 2005, pp. 422-432.

[4] E.J. O'Sullivan, C. E.I., L.T. Romankiw, K.T. Kwietniak, P.L. Trouilloud, J. JHorkans, C.V. Jahnes, I.V. Babich, S. Krongelb, H. S.G., J.A. Tornello, N.C. LaBianca, J.M. Cotte, and T.J. Chainer, "Integrated variable-reluctance magnetic minimotor," *IBM J. Research and Development*, vol. 42, no. 5, 1998.

[5] R.M. Bozorth, *Ferromagnetism*, Wiley-IEEE Press 1993.

[6] J.-M. Quemper, S. Nicolas, J.P. Gilles, J.P. Grandchamp, A. Bosseboeuf, T. Bourouina, and E. Dufour-Gergam, "Permalloy electroplating through photoresist molds," *Sensors and Actuators A: Physical*, vol. 74, no. 1-3, 1999, pp. 1-4.

[7] D.G. Jones, and A.P. Pisano, "Fabrication of ultra thick ferromagnetic structures in silicon," *ASME International Mechanical Engineering Congress and Exposition,* Anaheim, November 13-19, 2004.

[8] J.W. Judy, "Batch-fabricated ferromagnetic microactuators with silicon flexures," Mechanical Engineering, Univerisity of California, Berkeley, 1996.

[9] H.V. Venkatasetty, "Electrodeposition of thin magnetic permalloy films," *J. Electrochemical Society*, vol. 117, no. 3, 1970, pp. 403-407.

[10] X. Li, T. Abe, Y. Liu, and M. Esashi, "Fabrication of high-density electrical feed-throughs by deep-reactive-ion etching of pyrex glass," *J. Microelectromech. Syst.*, vol. 11, no. 6, 2002, pp. 625-630.

[11] T. Abe, X. Lia, and M. Esashi, "Endpoint detectable plating through femtosecond laser drilled glass wafers for electrical interconnections," *Sensors & Actuators A-Physical*, vol. 108, no. 1-3, 2003, pp. 234-238.

[12] S.D. Leith, and D.T. Schwartz, "In-situ fabrication of sacrificial layers in electrodeposited NiFe microstructures," *J. Micromech. Microeng.*, vol. 9, 1999, pp. 97-104.

[13] M.C. Wurz, D. Dinulovic, and H.H. Gatzen, "Investigation of permeability on electroplated and sputtered permalloy," *206ndMeeting of The Electrochemical Society,* Honolulu, October 3-8, 2004.